

Design of a Gravity Stabilised Fixed Pitch Tidal Turbine of 400kW

C. Freeman¹, J. Amaral Teixeira¹, F. Trarieux¹, R. Ayre²

¹ School of Engineering,
Cranfield University,
Cranfield, Bedfordshire, UK, MK43 0AL
E-mail: c.freeman@cranfield.ac.uk

² Tidal Energy Limited,
Vision House, Oak Tree Court
Mulberry Drive, Cardiff Gate Business Park, Cardiff, CF23 8RS
E-mail: rgayre@googlemail.com

Abstract

This paper describes the design of a fixed pitch horizontal axis tidal turbine for use in a DeltaStream device. The DeltaStream unit consists of three turbines each mounted on a swivelling nacelle atop a pylon which is located at the vertex of a delta shaped freestanding structure. The tidal turbine has to be designed so that the total thrust on the assembly is less than the frictional forces opposing any motion. This leads to a design requirement where the power-thrust ratio is a maximum for the turbine. This is especially difficult with a fixed pitch turbine where it is required to maximise the power over the tidal cycles for a maximum possible thrust. The turbine blades were designed using design methods more commonly used in turbomachinery rather than the Blade Element Method (BEM) used in wind turbines. The design was then assessed by CFD using CFX over a range of tip speed ratios to generate a set of non-dimensional characteristics which could be used, together with a tidal probability distribution from EMEC, to generate average powers and peak loads. The unsteady loads were assessed by estimating the level of the mean unsteady velocity and how the rotor would respond in a one-dimensional manner. Site specific data could then be applied to obtain more realistic loads.

Keywords: Fixed pitch, Freestanding, Tidal turbine.

Nomenclature

C	= coefficient, chord
F	= force
V	= velocity
μ	= friction coefficient
ω	= rotational velocity

Subscripts

a	= axial
p	= power
rel	= relative
t	= thrust
x	= longitudinal
D	= drag
L	= lift

Acronyms

BEM	= blade element momentum
CFD	= computational fluid dynamics
RPM	= rotations per minute
TSR	= tip speed ratio

1 Introduction

The most predictable form of renewable energy is tidal energy driven by the rotation of the Sun, Earth and Moon, and unaffected by clouds, atmospheric motion or day and night. To harness this energy two main types of device have been considered: barrages where water is impounded and let in and out through a turbine or turbines, the turbines having an enclosed rotor; or open rotor turbines placed in narrow passages between two large volumes of water. The first concept utilises the potential energy of the tides, the latter its kinetic energy.

The open rotor is subject to velocities induced by surface waves and unsteady velocities due to turbulence and the lower frequency velocities induced by the influence of local geometry on the tide.

Tidal turbines can either be fixed to the sea bed or held in place by their own weight and the friction of the seabed. Because the tide changes direction every 6 hrs or so, the rotor has to change pitch by approximately 180 degrees or the rotor and nacelle have to rotate 180 degrees to point into the flow. In addition the rotor has

to be designed to prevent cavitation damage to its blades.

Variable pitch mechanisms though complex have many benefits but in this project it was decided that fixed pitch turbines should be more reliable in the harsh undersea environment.

This paper describes the design of a fixed pitch horizontal axis tidal turbine for use in a DeltaStream device. The DeltaStream unit, developed by Tidal Energy Limited, consists of three turbines each mounted on a swivelling nacelle atop a pylon which is located at the vertex of a delta shaped freestanding structure, Fig. 1. The unit rests on the sea bed on three feet resulting in a stable structure akin to the traditional milking stool. The unit is deployed and recovered by a floating crane.

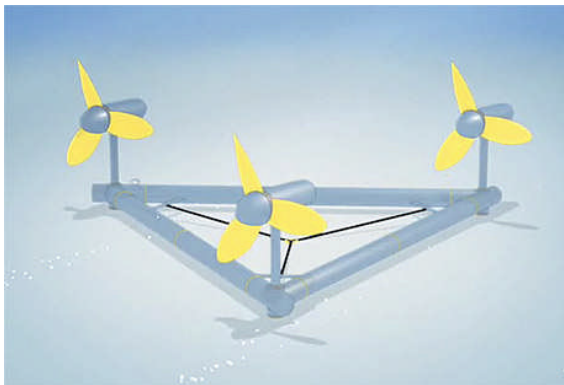


Figure 1: Schematic representation of a DeltaStream tidal device

This paper is concerned with the hydrodynamic performance and the estimation of loads for subsequent detailed mechanical design.

2 Design mission

A turbine is designed to perform a mission. It is required that the parameters of this mission be clearly defined: what velocities will it be exposed to, what extreme loads will it be exposed to and how much power will it be able to generate in a year. The tidal conditions assumed in this study were those of EMEC as described in [1]. This data is averaged over several minutes.

The turbine diameter and rotational speed must be chosen to maximise the annual energy output. The turbine must operate in unsteady flows such as those induced by surface waves and turbulence created by the tide flowing over the seabed without the freestanding frame moving.

3 Hydrodynamic design constraints

The four main design constraints are:

Frictional resistance: the assumed device weight is 250 tonnes in air and the effective friction coefficient $\mu=0.75$ with a 1.35 safety factor. The maximum axial load on the structure must not exceed the available

friction. This is a maximum thrust of 40.5 tonnes thrust per turbine.

Cavitation: deemed to be extremely unlikely at the conditions in which the turbines operate.

Close down time due to extreme loads: to be minimised. It was assumed that in the event of exceptionally high velocities induced by large surface waves or abnormal tidal surges the rotors can be furled to reduce the drag if required.

Power rating: 400 Kilowatts.

4 Choice of tip speed ratio

Wind turbines are typically designed for tip speed ratios (TSR) around 6. That is, the tip peripheral speed is 6 times the wind speed. This in general maximises the power for a given diameter.

The major constraint for the type of tidal turbine described in this work is that the total drag must be less than the available friction force at all times. To determine which TSR would give the greatest power for a given drag, calculations were made for a range of two-dimensional designs at different tip staggers over a range of tip speed ratios using the BEM method described in [2].

Results are shown in Fig. 2 where the coefficients of power and thrust, C_p and C_t , are plotted for 3 tip staggers from 2 to 10 degrees. The stagger quoted is the angle of the aerofoil to the tangential direction. The closer to tangential the greater the TSR.

It can be seen that at low staggers the turbine thrust is higher when unloaded than when loaded so that low stagger blades are not desirable as, should the grid connection fail, the thrust will in these cases increase.

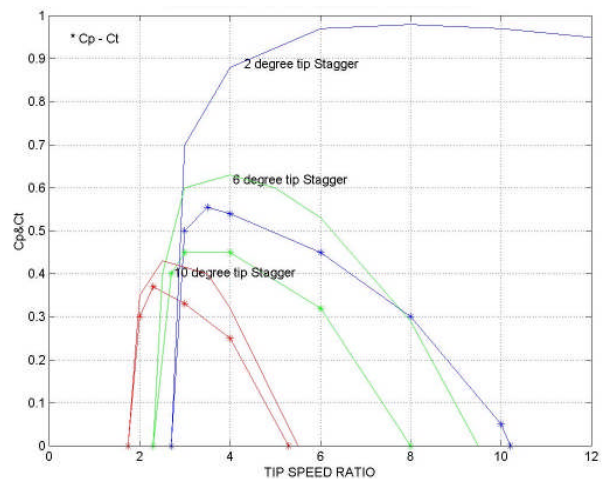


Figure 2: Power and thrust coefficients for a range of blade tip staggers

In terms of drag it can be seen in Fig. 2 that as stagger increases and TSR falls the ratio of C_t/C_p max falls, so the drag for a given power falls. The drag at no load falls and the speed increase from full power to no power reduces. Low TSR has therefore many benefits for the type of tidal turbine being designed although the size of a turbine for a given power increases. Cavitation

is also improved at low TSR since larger chords and low relative velocities increase the minimum static pressure. The blade unsteady response will be reduced by the higher Reduced Blade Frequency (fC/V_{rel}) as the chord, C , is increased whilst V_{rel} is reduced.

5 Rotor design

The design process employed differs from that of most wind turbines, such as described by [3], in that it uses the throughflow calculation methods due to [4]. It is used to determine the relative velocities on to the rotor in the same way that [5] used in the design of an open rotor. This is the process used in turbomachinery with casings and is well understood by the authors. It represents a 2D solution where pitchwise variations are small, and it models the change in streamtube area. The outer boundary is found iteratively to give a nearly constant static pressure. Output from the calculation is shown in Fig 3 where the values of meridional velocity and position of the mean streamlines are shown against axial position and radius in meters.

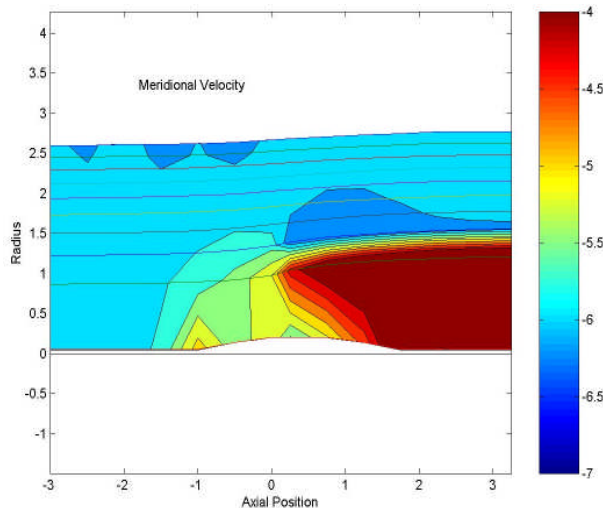


Figure 3: Throughflow prediction for a 1m radius turbine

As in [5] the rotor is set up in a duct with a jump condition in tangential velocity across the rotor to give the required work. The rotor work is the rotational speed times torque and the torque is the radius times the change in angular momentum. The nacelle is included to obtain the influence of the nacelle shape on the blade relative velocity. This particular calculation method would not handle a zero radius so a small diameter tube was imposed on the axis.

The figure shows the familiar increase of stream tube area in the flow direction and the reduction of flow velocity as the flow approaches the rotor and through the rotor.

The calculation shows the change in mean streamlines, the curvature of the streamlines near the rotor and the velocity drop in the wake. It also shows that the nacelle curvature alters the meridional velocity. The velocities obtained from the throughflow analysis and the blade element performance as computed from

[6], together with the Prandtl Tip Loss Factor from [2], enables the blade geometry to be defined.

A series of designs with the same change of total pressure for a range of TSR and mean blade chord were investigated to allow the best design to be selected. Selection could be made on the basis of minimum size, minimum thrust at a power or most margin above cavitation.

The turbine had 3 blades; fewer blades leads to higher tip losses and more blades to less robust blades. The tip speed ratio chosen is that with the lowest drag to power ratio. Fig 4 shows that for a tidal flow of 3 m/s the best drag to power ratio occurs with a TSR=3.2 and a chord of 1.8 m for a nominal 15 metre diameter turbine. The highest value of C_p occurred with a tip speed ratio of just over 5.

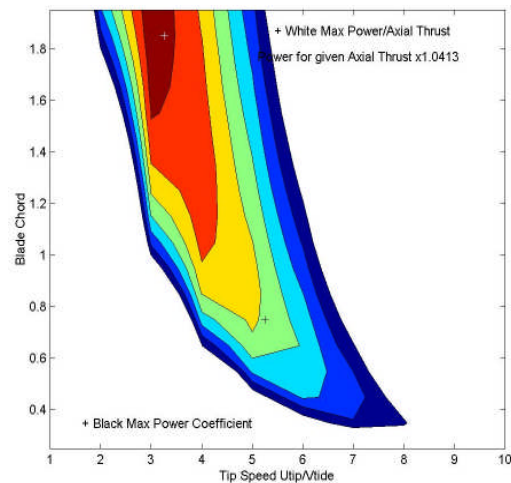


Figure 4: Power coefficient divided by thrust coefficient

6 Choice of blade section

It is customary to design an aerofoil with camber as this increases the blading efficiency. The ratio of C_L to C_D is a measure of this blading efficiency and, as can be seen from Fig 5, this is higher with a cambered blade. However in this device the power-off performance is the most important consideration and the choice was thus made to employ an uncambered aerofoil. This solution minimises the power-off thrust and any blade stalling problems at high tidal flows when the blades are unloaded and running at a higher rotational speed.

The design selected for minimum thrust at a given power was then calculated in a constant area duct in the CFD code CFX over a range of tidal flows and a set rotational speed. The constant area duct was used since it is not until the calculation is carried out that the exact stream tube areas are known.

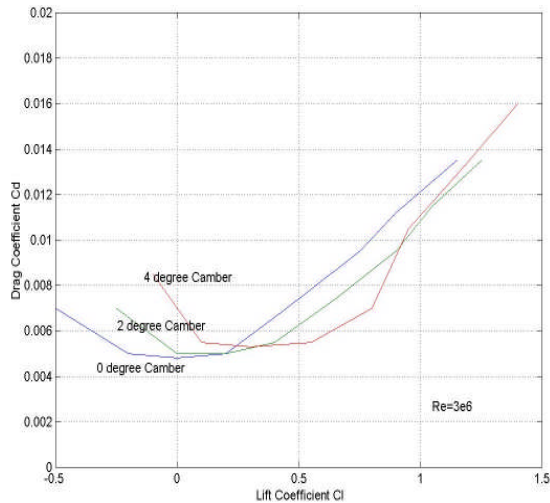


Figure 5: Performance of NACA 63 series aerofoils

Some of the output from the CFD is shown below. The C_p curve derived from the CFD computations is compared with the design intent value in Fig 6.

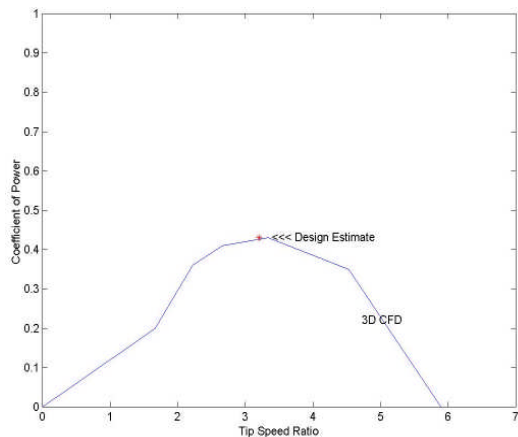


Figure 6: Comparison between CFD predictions and design intent

The correction of the data obtained from the constant area CFD model was performed as in [7].

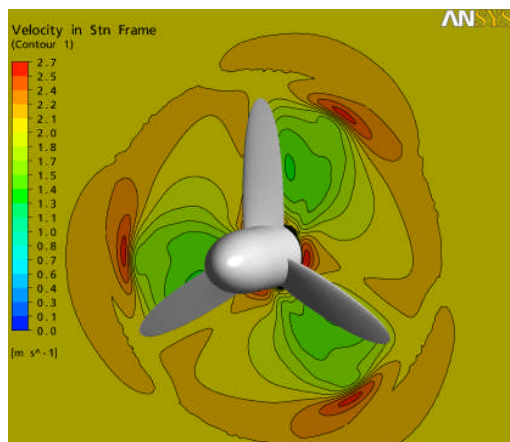


Figure 7: Velocity in stationary frame downstream of the turbine

The plot in Fig 7 shows the absolute velocity downstream of the turbine at 9.2 RPM and an inflow velocity of 2.0 m/s.

As is apparent in this plot there are pockets of higher velocities associated with the tip region but these peaks are modest in extension and relatively weak in intensity due to the configuration of the blade tips.

The following two figures show the relative velocity vectors superimposed on the static pressure field at 70% of the blade span.

In the first of these plots, Fig 8, a low flow simulation for 9.2 RPM and 1m/s tidal speed corresponding to a tip speed ratio of 7 is shown. This situation is close to the freewheel condition and shows how flow is well attached and so is unlikely to induce buffeting should the turbine freewheel a circumstance which should only occur at high tidal speeds or when grid connection is lost.

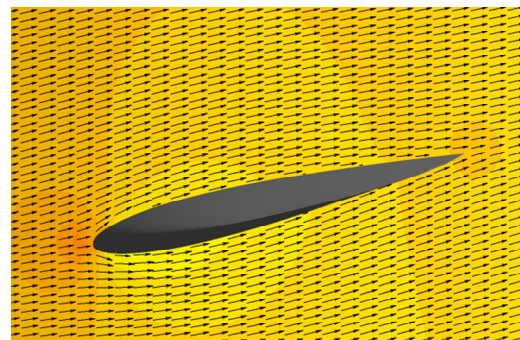


Figure 8: 70 % span (low flow)

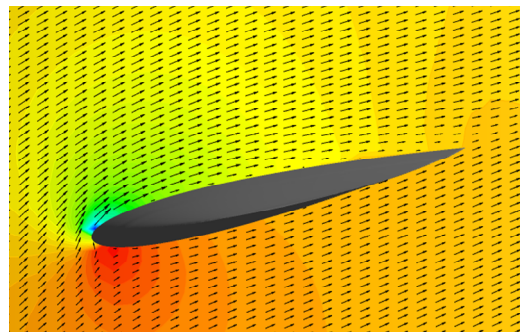


Figure 9: 70 % span (high flow)

The high flow simulation, Fig 9, was computed at 9.2 RPM and 3 m/s giving a TSR of 2.3, lower than intended in normal operation. The vectors show that the flow on the suction surface is close to separation at this condition.

The predicted thrust and torque curves for a 15m turbine are shown in Fig 10 and Fig 11. As well as the operating lines, loaded and unloaded, they show the fall off in thrust as the torque is reduced and the low thrust when the turbine is operating unloaded. The turbine operates at peak power up to rated power and at constant power thereafter.

7 Sizing the turbine

When the C_p and C_t curves are available the turbine can be sized for the proposed duty. The duty used was

that measured at the Fall of Warness site in the Orkneys [1]. The constraints are that the thrust for the 3 turbines plus the frame drag must not exceed $\mu \cdot 250$ tonnes with a safety factor of 1.35 at any tidal speed.

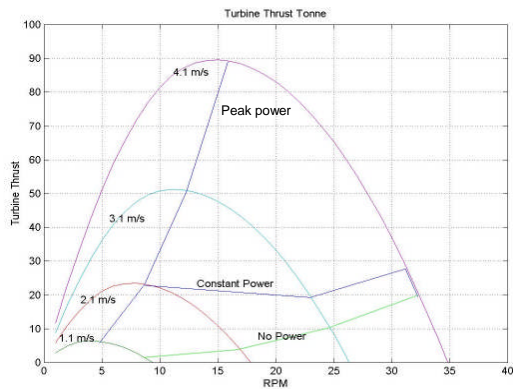


Figure 10: Turbine thrust (Ton)

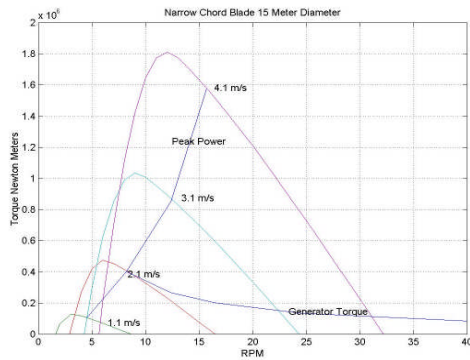


Figure 11: Turbine torque (Nm)

The overall annual average power is the sum of power at a tidal flow multiplied by the probability of that flow.

An optimisation for this mean annual power was performed by assuming that a range of machines was matched to peak C_p for a range of tidal speeds. The turbines were sized to give a thrust and hence a rated power. Each machine was run over the tidal range and the mean power obtained. If any machine exceeded the thrust requirement at any tidal flow it was resized to match the constraint. The results are seen in Fig 12 showing that best performance was obtained by matching for the most probable tides and running unloaded at high tidal speeds.

The optimum generator size, using the EMEC data, should result in about 50% annual electrical yield, expressed as the ratio of the average annual power to the rated power, for a 15m diameter turbine.

8 Unsteady loading

The level of unsteady loads that may be experienced by a tidal current turbine has been examined by [8]. His analysis indicates that the magnitude of the unsteady loads is comparable to that of the steady loads. In the case of the gravity stabilized tidal turbine the maximum

axial thrust is of major importance since the maximum thrust must not exceed the frictional drag.

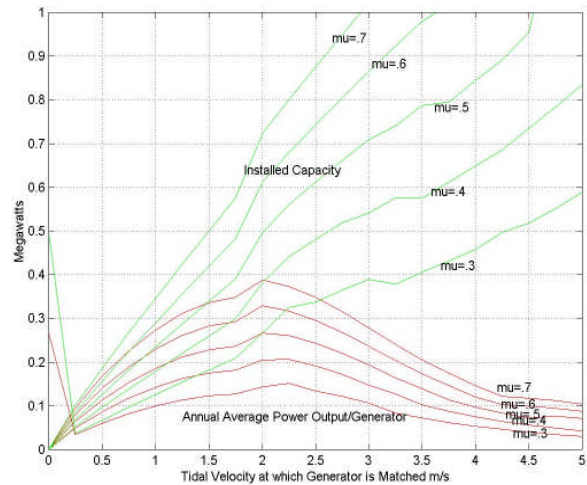


Figure 12: Generator optimization

Tidal turbines are subjected to unsteady loads from waves, turbulence, storm surges and reflections and refractions from irregular coasts and sea beds, etc. The turbine responds predominately to the axial velocity variation produced by the above. Tidal channel flows are boundary layer like having shear at the bottom and small wind shear at the top and have hence a boundary layer like profile typically approximated by a 1/7 power law. Consequently it is expected that they will have typical boundary layer turbulence and, since the turbine size is comparable to the expected length scales of turbulence, it will see the turbulence as loading changes.

The unsteady loads can be divided into 2 types:

- 1 - Unsteady force or torque applied to the structure by the turbine.
- 2 - Unsteady loads on individual blades that produce no major overall changes in axial thrust or torque but may contribute to other moments.

These loads can be separated by examining the Fourier components of the turbine face axial velocity.

The axial thrust and torque applied to the structure is the sum of the loads on all three blades. The blades acted upon by any circumferential axial velocity component will differ in phase by ± 120 degrees multiplied by the harmonic number. Only a few components will give a non-zero net load.

Zero order components affect torque and thrust, 1st and 2nd components do not. Conversely 3rd and 6th components for a 3 bladed rotor do. On the other hand 1st and 2nd components produce net out of plane bending but 3rd and 6th components do not.

To investigate torque and axial thrust variations it is the zero order forces that will be most important. These can be accounted for by looking at the variation of the circumferentially mean inflow velocity over the rotor.

This rotor has a near constant chord except near the tip and the blade section axial force and torque variation with inlet flow are hence proportional to radius. dF_x/dV_a and $dTorque/dV_a$ are also proportional

to radius except close to the tip so the total axial force and torque is the radial integral of the zeroth circumferential component of the upstream velocity.

The radial integral of the zeroth order circumferential component is close to the area mean value, if the 3rd, 6th, circumferential terms, etc are small compared with the zeroth order. In this case estimation of the area mean velocity fluctuation upstream of the rotor will provide a reasonable estimate. In the design a more precise method [9] was used.

An increase in torque will result in an acceleration of the turbine with an increase in rotational speed resulting in a change of tip speed ratio. To account for these effects it is necessary to examine the response of the turbine to an oscillating flow over a range of frequencies from 0.001 to 5Hz. This was done by assuming that the steady state performance was modified by a Sears function [10]. This obviously could only be used for attached flows and not when the rotor was stalled. However the rotor only nears stall at low tidal flows. The turbine torque/flow/speed characteristic was used with a one-dimensional sinusoidal tidal velocity fluctuation to generate a torque applied to the transmission and generator.

The turbine torque-generator torque equals $I d\omega/dt$ where I is the moment of inertia of the turbine generator and drive train referred to the turbine shaft. A MATLAB differential equation solver then computes the resulting RPMs for the sequence. The process is insensitive to initial guess if the calculation is carried out for a number of cycles. The response to oscillating flow was calculated for a range of mean velocities and over a range of frequencies from 0.01 to 1Hz and for amplitudes of 10% and 20% of the time mean flow. The generator torque was assumed to be that for peak power up to the rated power and then constant power.

Results are shown in Fig 13. These show that for an inertia referred to the turbine shaft of 400,000 Kg^m², below 0.01 Hz the device is insensitive to oscillations but at 0.1 Hz, or wave frequencies, it is sensitive and it is very sensitive to frequencies around 1Hz. At higher frequencies the sensitivity falls off. These calculations are for plane waves.

Measurements of unsteady velocities from specific sites can then be incorporated in the model when available. In the case of this gravity stabilised tidal turbine the whole stability of the device will be determined by the worst unsteady axial load which has to be less than an average of 40.5 tonnes axial load per rotor to meet the chosen safety margin.

The turbine and generator combination in an oscillating flow show significant increases in axial thrust and variations in torque and the response to unsteady flows is critical to the design.

When the turbine experiences an increase in inflow velocity the torque increases and the axial thrust increases. The torque causes the turbine shaft, gearbox and generator to accelerate. As the RPM increases the torque falls so the response depends on how the turbine rotational speed changes with the changing inflow.

The values of these unsteady loads are dependent on the site-specific tidal velocity, waves and random unsteadiness.

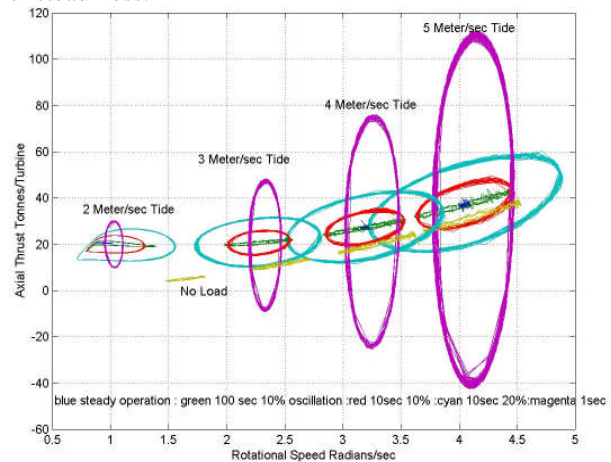


Figure 13: Frequency response of turbine to oscillatory flow

For design ‘typical’ data must be used. However it can be seen that the maximum design axial thrust 40.5 tons is almost reached in steady state at 5 m/s tidal flow. The maximum tidal speed that could be used with an unsteady velocity of 20% of the mean is 4m/s so high tidal speeds are not suitable for this machine.

9 Design options for controlling unsteady loads

Turbulence and waves are not in the gift of the turbine designer but other features, relevant to the operation of the turbine, are.

The calculations were re-run with an inertia of 1,000,000 Kg^m². Employing this higher inertia doubled the unsteady loads at 0.1 Hz, a typical wave frequency, for the same velocity perturbation. Recalculated with zero inertia the turbine had no unsteady axial load. The lower the inertia the less axial load that has to be designed for. These calculations were all performed with an unsteady generator torque/speed relationship which was the same as used for the steady state curve.

To examine the influence of the generator the loads were recomputed with datum inertia and a synchronous generator synchronised to the mains. This produced unsteady axial loads that were three times as high as for the nominal inertia with the same velocity perturbation.

The mechanical and electrical design of the machine is of utmost importance with a gravity-stabilised turbine. If the generator design results in a large unsteady load then the maximum tidal speed the machine can operate in, will have to be reduced. The designer’s major means of reducing unsteady axial loads are low inertia and soft electrics.

10 Estimation of wave-induced velocities

Falnes, [11], shows the relationship between height and time period of surface gravity waves and the velocity induced by surface waves travelling along a

constant depth channel. The area mean velocity over the rotor face can be calculated and applied to the upstream boundary. The amplitude of the 3rd order harmonics can be shown to be negligible. The change in axial thrust will result in an equal and opposite force on the wave but for realistic turbine area/channel area the change in rotor thrust is small compared to the peak axial momentum of the wave.

The calculation can be made for a range of wave heights and periods such as described by [12] and a statistical description of the forces can be generated for extreme load and fatigue load assessment. An example is shown in Fig 14 where the mean velocities induced by the waves are shown superimposed on a ‘Scatter Diagram’ from [12].

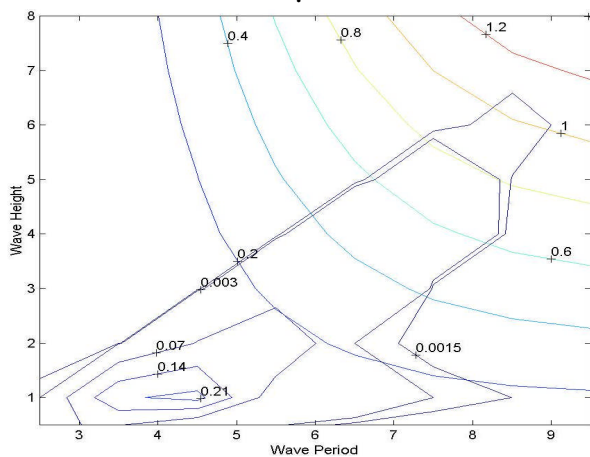


Figure 14: Wave climate employed in study with superimposed lines of wave-induced velocities

11 Estimation of turbulent velocities

McCann [8] describes a model for the estimation of time varying velocities from the natural turbulence generated by the tidal movement over the seabed, derived from a modified atmospheric model. However to estimate the maximum loads and fatigue loads a statistical model is required. The method used is described in [9] but is outside the scope of this paper. Here the maximum effective turbulent velocity will be taken as 0.18 times the tidal speed with a frequency of 0.05 Hz since these are typical values from [12].

12 Estimation of wave-induced velocities

Overall loads are due to combinations of tidal velocity, wave height and times and turbulence in the channel. The proportion of the required operating life spent at any tide speed and sea state is the product of the probability of the tide speed and the probability of that sea state. The turbulent loading for any combination of tidal speed and sea state will depend on time spent at that condition. In this case we assume that the same level of turbulence applies. The total load can then be calculated for all combinations of tidal speeds

and waves and a matrix of tidal speeds and wave induced speeds can then be produced.

Each point on the matrix has a time spent, a steady load, a wave induced load and a turbulent load. The total load is the sum of these quantities and the fatigue load corresponds to their amplitude and number of reversals. The extreme load is the largest.

These extreme and fatigue loads are used to design the turbines. The tidal data and wave data can be scaled; this enables the design to be run over a range of sea states and tides to determine the operating envelope.

Data from the calculation is shown in Fig 15 below. Here the axial force is shown for all tidal speeds and sea states from the EMEC data [1] for the tides and Nielsen [12] for the waves. The turbulent velocities were input as a fixed proportion of the tidal speed but in reality the maximum turbulent velocity would be larger for the high probability states than the low probability states. The maximum load with a large tidal velocity and a severe sea state is around 57 tonnes. The maximum average of the 3 rotors is lower since turbulence and waves due not impact all 3 rotors simultaneously and that is estimated to be 52 tonnes greater than the design loading with the 1.35 safety factor of 40.5 tonnes. Fig 15 shows that the axial thrust drops when the generator is unloaded by 12 tonnes at 4 m/s tidal speed. This target can be achieved with intelligent control. These wave climate and tidal speeds are severe and many sites should be more benign.

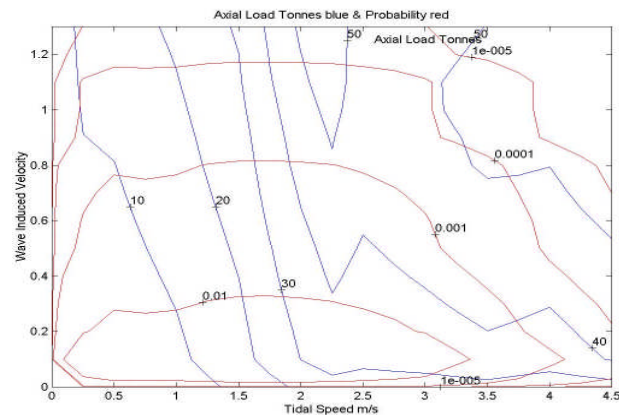


Figure 15: Axial loads with probability of occurrence

13 Conclusions

Although tidal energy is predictable and dependable the loads acting on an open rotor tidal turbine are not and can only be estimated statistically.

A design procedure has been established to design tidal turbines that are free standing.

A methodology has been developed to estimate the unsteady loads when site specific data is available to be fed into the model.

Acknowledgements

The authors express their gratitude to Tidal Energy Limited for their permission to publish this paper. Thanks are also due to Chirath Assalaarachchi who run the CFD simulations as part of his doctoral program at Cranfield University.

References

- [1] G. T. Melville, S. Couch, I. Bryden. Hydrodynamic Modelling and Survey Data Analysis for the Fall of Warness, Eday, Orkney. The Robert Gordon University, 2005.
- [2] M. O. L. Hansen. Aerodynamics of Wind Turbines. Earthscan, Chapter 6, 45:62, 2008.
- [3] W. M. J. Batten, A. S. Bahaj, A. F. Molland, J. R. Chaplin. The prediction of the hydrodynamic performance of marine current turbines. *Journal of Renewable Energy*, 33:1085-1096, 2007.
- [4] J. D. Denton. Throughflow calculations for transonic axial flow turbines. *ASME J. Eng. Power*, 100:212-218, 1978.
- [5] L. H. Smith. Unducted fan aerodynamic design. *Journal of Turbomachinery*, 109(3):313-324, 1987.
- [6] P. C. Klimas. Tailored airfoils for vertical axis wind turbines, Sandia Report, Sandia 84-1062, UC-60, 1992.
- [7] A. S. Bahaj, A. F. Molland, J. R. Chaplin and W. M. J. Batten. Power and thrust measurement of marine current turbines under various hydrodynamic flow conditions in a cavitation tunnel and a towing tank. *Journal of Renewable Energy*, 32:407-426, 2007.
- [8] G. N. McCann. Tidal current turbine fatigue loading sensitivity to waves and turbulence – a parametric study. Proceedings 7th EWTE Conference, Porto, 2007.
- [9] C. Freeman, I. J. Day and J. Amaral Teixeira. The use of small-scale hot wire experiments to estimate the loading of tidal turbines due to steady and unsteady flow variations. To be published.
- [10] H. H. Hubbard. Aeroacoustics of Flight Vehicles, Theory and Practice, Volume 1: Noise Sources. Acoustic Society of America, 1994.
- [11] J. Falnes. Ocean waves and oscillating systems: linear interactions including wave-energy extraction. Cambridge University Press, 2002.
- [12] K. Nielsen. Scatter diagram for Horns Rev. I.E.A. Ocean Energy Systems. Annex 11, p31, Table 2.2 (30 metres depth of Danish Coast).